

Supporting Information

EGFR Binding Fc Domain-Drug Conjugates: Stable and Highly Potent Cytotoxic Molecules Mediate Selective Cell Killing

Sebastian Jäger^{*[b,a]}, Stephan Dickgiesser^[a], Jason Tonillo^[a], Stefan Hecht^[a], Harald Kolmar^[b] and Christian Schröter^{*[a]}

[a] S. Jäger, Dr. S. Dickgiesser, Dr. J. Tonillo, Dr. S. Hecht, Dr. C. Schröter
ADCs & Targeted NBE Therapeutics, Merck KGaA, Frankfurter Str. 250, 64293 Darmstadt, Germany
E-mail: christian.a.schroeter@merckgroup.com, sebastian.jaeger@merckgroup.com

[b] S. Jäger, Prof. Dr. H. Kolmar
Institute for Organic Chemistry and Biochemistry, Technical University of Darmstadt, Alarich-Weiss-Str. 4, 64287 Darmstadt, Germany

Table of Contents

1. Amino acid sequences of expressed proteins.....	3
2. Purification of antibody fragments	5
3. Analytics of antibody fragments	6
4. Biological evaluation of antibody fragments.....	8
5. Cellular uptake assay	10
6. Generation of MMAE conjugates.....	17
7. Analytics of MMAE conjugates.....	18
8. Receptor binding properties of MMAE conjugates.....	21
9. References.....	23

1. Amino acid sequences of expressed proteins

Fcab-1 (modified FS1-60^[1]):

APELLGGPSVFLFPPKPKDLMISRTPEVTCVVVA^ΔVSHEDPEVKFNWYVDGVEVHNAKTKPREEQ^ΔYNSTYRVVSVLTVL
HQDWLNGKEYKCKVSNKALPAPIEKTISKAKGQPREPQVYTLPPSRDELDEGGPVS^ΔLTCLVKGFYPSDIAVEWESTYGPE
NNYKTPPVLDSDGSFFLYSRLTVSHWRWYSGNVFSCVMHEALHNHYTQ^ΔKLSLSPG

Fcab-2 (modified FS1-65^[1]):

APELLGGPSVFLFPPKPKDLMISRTPEVTCVVVA^ΔVSHEDPEVKFNWYVDGVEVHNAKTKPREEQ^ΔYNSTYRVVSVLTVL
HQDWLNGKEYKCKVSNKALPAPIEKTISKAKGQPREPQVYTLPPSRDELDEGGPVS^ΔLTCLVKGFYPSDIAVEWESTYGPE
NNYKTPPVLDSDGSFFLYSKLTVSYWRWVKGNVFSCVMHEALHNHYTQ^ΔKLSLSPG

Fcab-3 (modified FS1-67^[1]):

APELLGGPSVFLFPPKPKDLMISRTPEVTCVVVA^ΔVSHEDPEVKFNWYVDGVEVHNAKTKPREEQ^ΔYNSTYRVVSVLTVL
HQDWLNGKEYKCKVSNKALPAPIEKTISKAKGQPREPQVYTLPPSRDETDDGPVS^ΔLTCLVKGFYPSDIAVEWESTYGPEN
NYKTPPVLDSDGSFFLYSKLTVSYWRWYKGNVFSCVMHEALHNHYTQ^ΔKLSLSPG

huFc (modified human IgG1 Fc fragment):

TCPPCPPELLGGPSVFLFPPKPKDLMISRTPEVTCVVVA^ΔVSHEDPEVKFNWYVDGVEVHNAKTKPREEQ^ΔYNSTYRVV
SVLTVLHQDWLNGKEYKCKVSNKALPAPIEKTISKAKGQPREPQVYTLPPSRDELTKNQVSLTCLVKGFYPSDIAVEWES
NGQPENNYKTPPVLDSDGSFFLYSKLTVDKSRWQQGNVFSCVMHEALHNHYTQ^ΔKLSLSPG

C-IgG (Cetuximab modified with LC C-terminal (G₄S)₃-LPETGS sortase A recognition tag for conjugation):

Light chain

DILLTQSPVILSVSPGERVSFSCRASQSIGTNIHWYQQR^ΔTNGSPRLLIKYASESISGIPSRFSGSGSGTDFTLSINSVESEDIAD
YYCQQNNNWPTTFGAGTKLELKRVAAPSVFIFPPSDEQLKSGTASVVCLLNNFYPREAKVQWKVDNALQSGNSQESV
TEQDSKDYSLSTLTLSKADYEKHKVYACEVTHQGLSPVTKSFNRGECGGGGSGGGGSGGGGSLPETGS

Heavy chain

QVQLKQSGPGLVQPSQSLITCTVSGFSLTNYGVHWVRQSPGKGLEWLGVIWSSGNTDYNTPTFTRLSINKDNSKSQV
FFKMNSLQSNDAIYYCARALTYDYEFAYWGQGLTVTVAASKGPSVFPLAPSSKSTSGGTAALGLVKDYFPEPVTV
SWNSGALTSGVHTFPAVLQSSGLYSLSSVTVPSSSLGTQTYICNVNHKPSNTKVDKRVKPKSCDKTHTCPPCPPELLG
GPSVFLFPPKPKDLMISRTPEVTCVVVDVSHEDPEVKFNWYVDGVEVHNAKTKPREEQ^ΔYNSTYRVVSVLTVLHQDWL
NGKEYKCKVSNKALPAPIEKTISKAKGQPREPQVYTLPPSRREEMTKNQVSLTCLVKGFYPSDIAVEWESNGQPENNYKTT
PPVLDSDGSFFLYSKLTVDKSRWQQGNVFSCVMHEALHNHYTQ^ΔKLSLSPGK

C-Fab (Cetuximab Fab fragment modified with LC C-terminal $(G_4S)_3$ -LPETGS sortase A recognition tag for conjugation and HC C-terminal G_4S -His₆ tag for purification):

Light chain

DILLTQSPVILSVSPGERVSFSCRASQSIGTNIHWYQQRRTNGSPRLLIKYASESISGIPSRFSGSGSGTDFLSINSVESEDIAD
YYCQQNNNWPTTFGAGTKLELKRTVAAPSVFIFPPSDEQLKSGTASVVCLLNNFYPREAKVQWKVDNALQSGNSQESV
TEQDSKDYSLSTLTLSKADYEKHKVYACEVTHQGLSSPVTKSFNRGECGGGGSGGGGSGGGGSLPETGS

Heavy chain

QVQLKQSGPGLVQPSQSLITCTVSGFSLTNYGVHWVRQSPGKGLEWLGVIWSSGNTDYNTPFTRSLSINKDNSKSQV
FFKMNSLQSNDAIYYCARALTYDYEFAYWGQGLVTVSAASTKGPSVFPLAPSSKSTSGGTAALGCLVKDYFPEPVTV
SWNSGALTSGVHTFPAVLQSSGLYSLSSVTVPSSSLGTQTYICNVNHKPSNTKVDKRVEPKSCDKTHTGGGGSHHHHH
H

D265A, **Q295**, Q311, Q438

2. Purification of antibody fragments

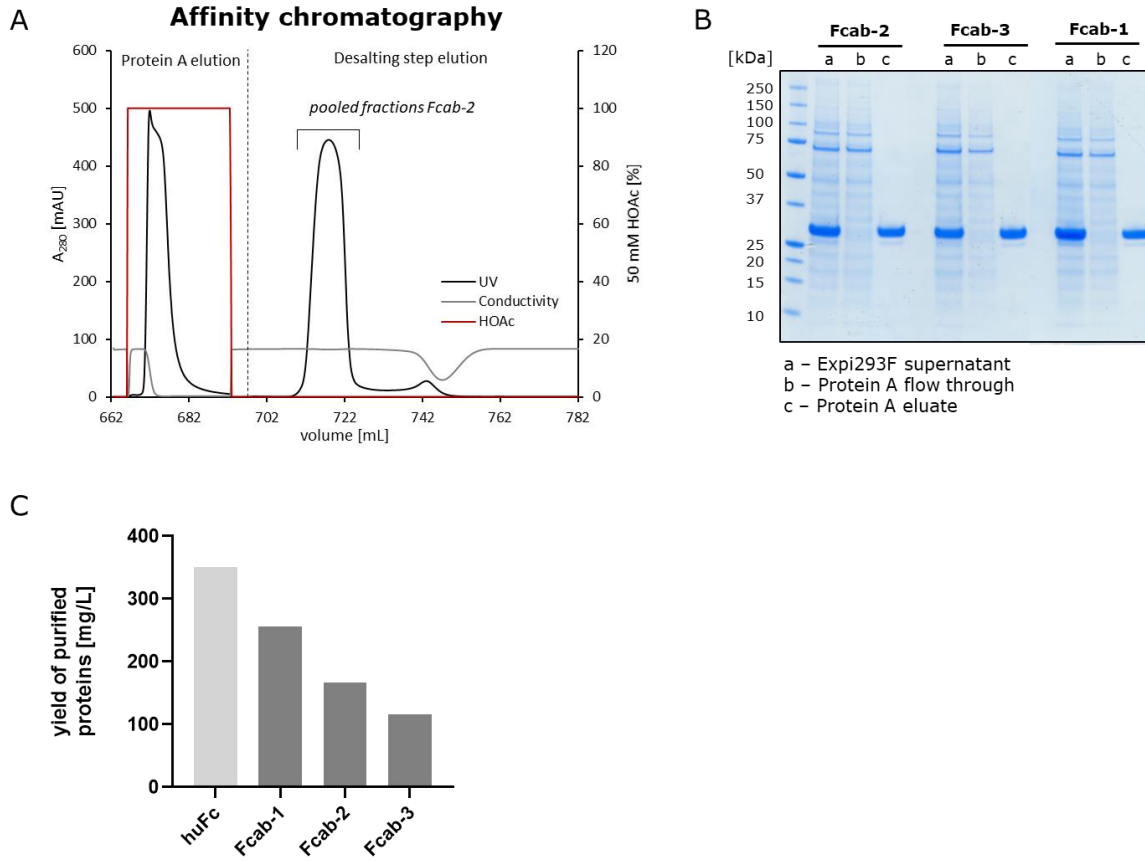


Figure S1. Protein A purification process of expressed Fcabs (**A**) Exemplary ÄKTA Xpress (HiTrap™ MabSelect SuRe™ 5 mL and HiPrep™ 26/10 desalting column) chromatogram showing Fcab-2 protein peak after elution from protein A column (50 mM acetic acid (HOAc), pH 3.2) and a second protein peak after a subsequent buffer change step. (**B**) SDS-PAGE analysis of reduced Expi293F supernatant, protein A flow through and purified Fcabs. 4-12 % Bis-Tris gel (Invitrogen™), MES SDS running buffer (1x), 40 min at 200 V, stained with InstantBlue™ (Coomassie-based) for 2h, marker: Precision Plus Protein™ Unstained Standards (BioRad). (**C**) Yields of purified Fcabs and huFc negative control per volume Expi-293F expression culture.

3. Analytics of antibody fragments

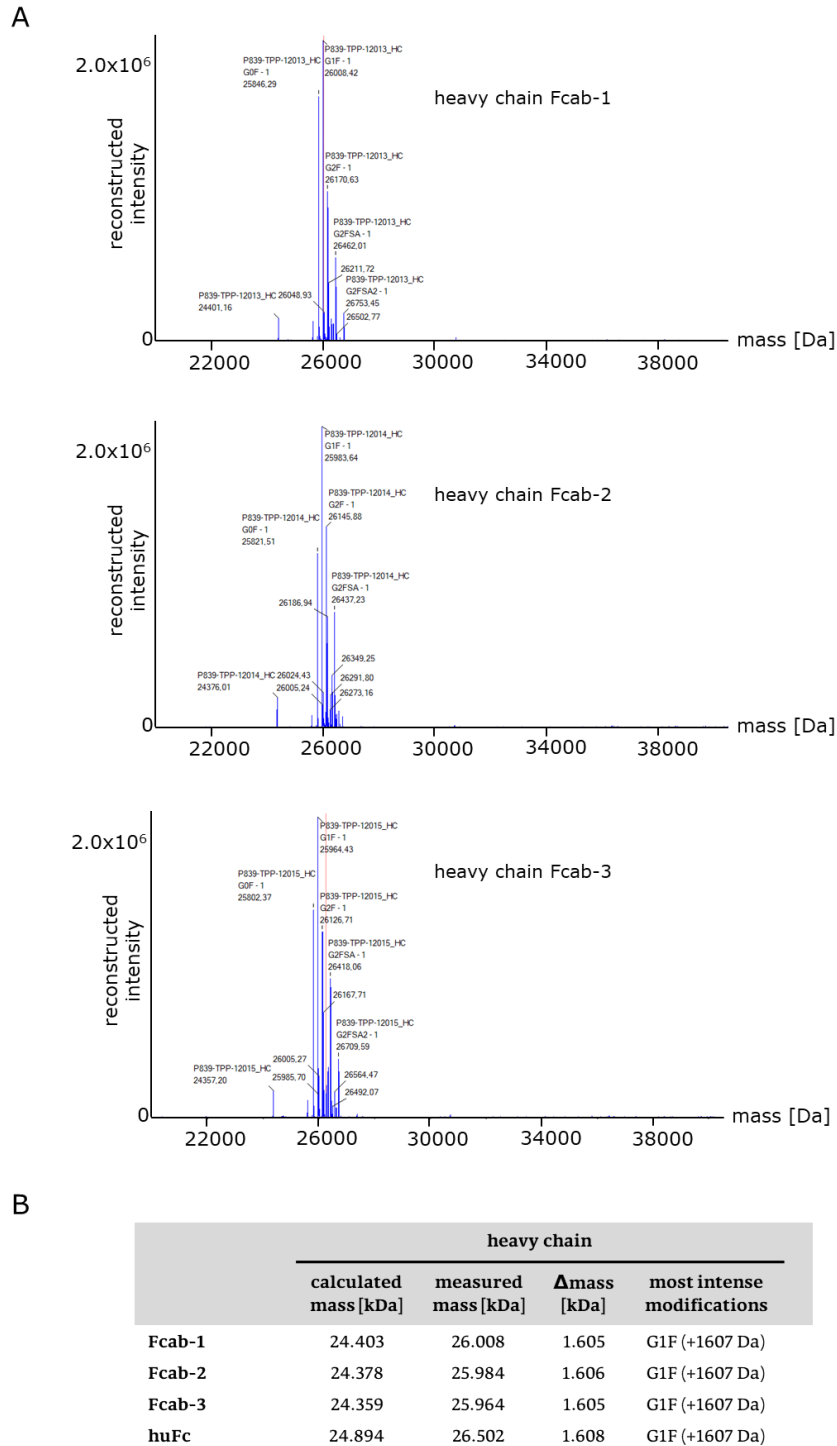


Figure S2. LC-MS analysis confirms the identity of Fcabs and huFc controls. **(A)** Deconvoluted MS spectra of Fcabs. **(B)** Mass variations between calculated and observed masses account for glycosylation patterns and standard measurement deviations. Only the most intense glycosylation pattern (G1F) is listed.

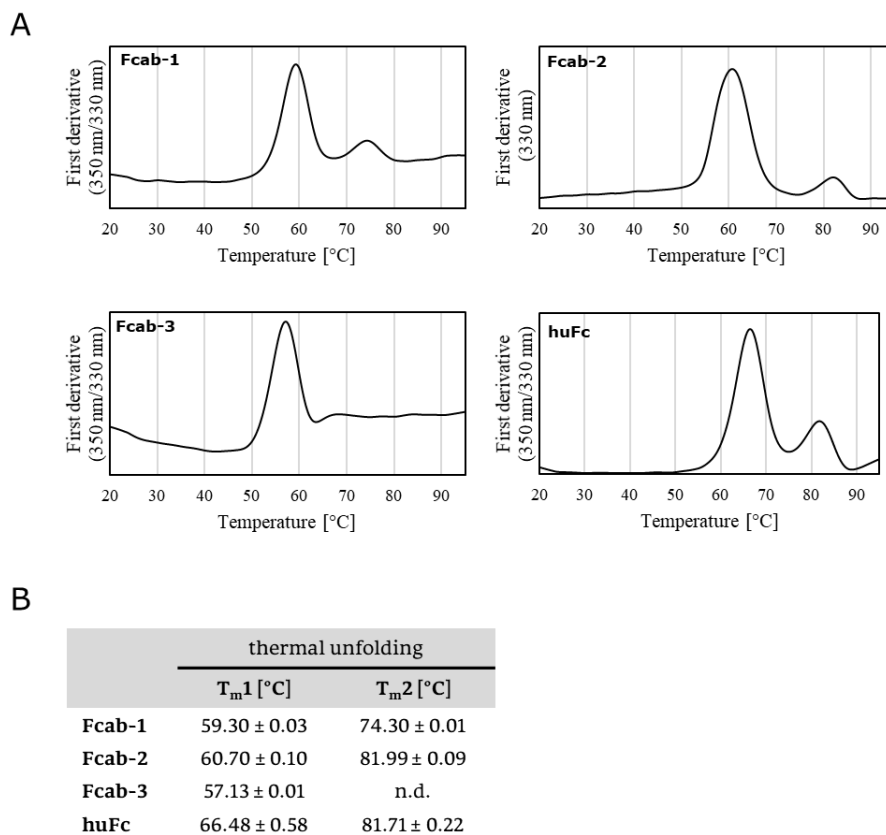


Figure S3. Thermal stability of Fcabs and huFc control molecule. The first derivative of thermal unfolding curves (**A**) as well as the unfolding transition midpoints (T_m) (**B**) are shown. To determine thermal unfolding, Fcabs and huFc (PBS pH 6.8) were loaded into nanoDSF grade standard capillaries which were then transferred into a Prometheus NT.PLEX nanoDSF (NanoTemper Technologies) instrument. Samples were subjected to a linear thermal ramp from 20 °C to 95 °C at a slope of 1 °C/min with simultaneous recording of fluorescence at 350 and 330 nm. Unfolding transition midpoints (T_m) were determined from the first derivative of the fluorescence ratio 350 nm/330 nm. All samples were measured in duplicates. n.d. – not detected

4. Biological evaluation of antibody fragments

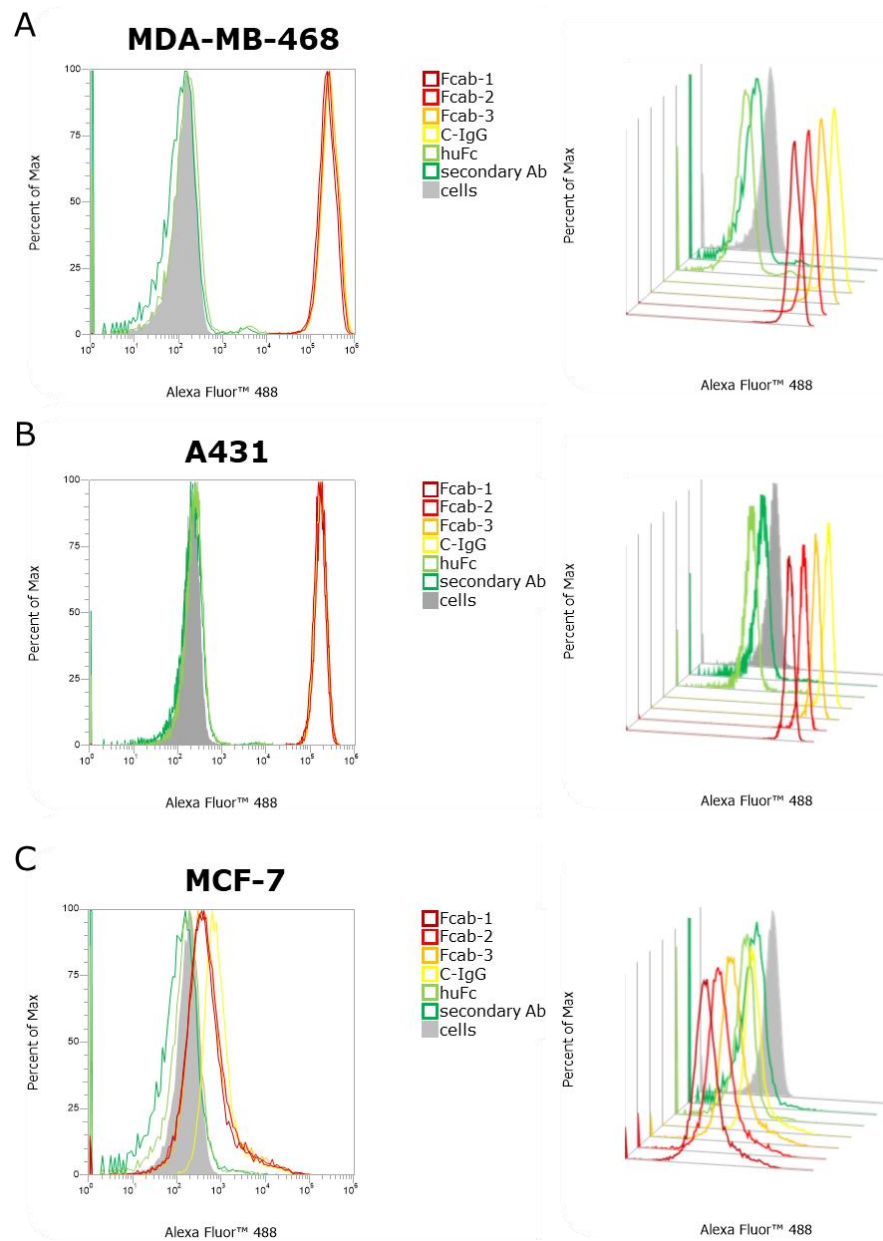
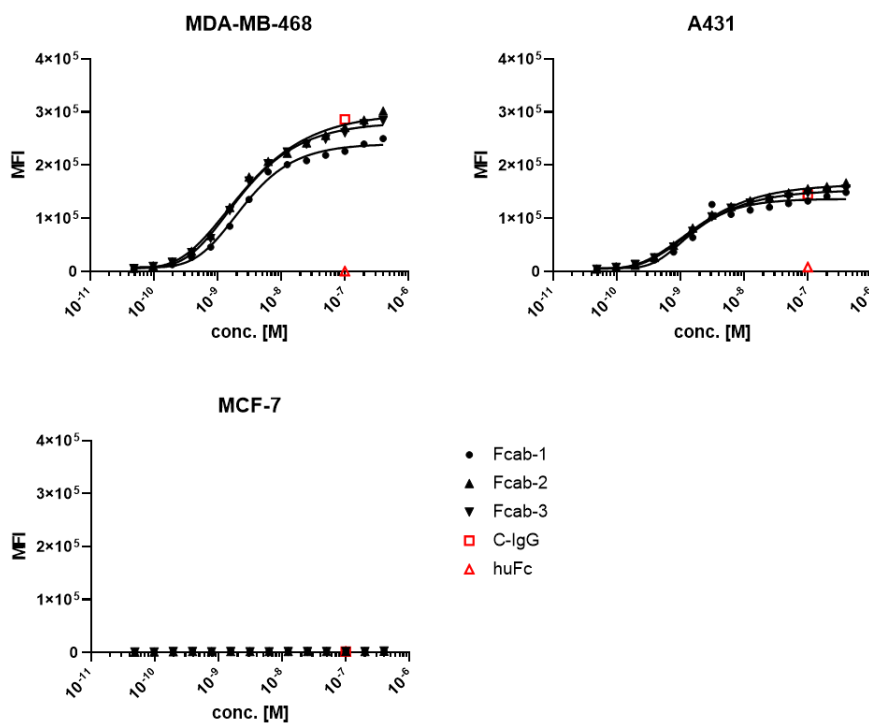


Figure S4. Cellular binding analysis of Fcabs and control molecules on EGFR positive (MDA-MB-468 and A431) and EGFR negative (MCF-7) cells. Fcabs and C-IgG bind selectively EGFR expressing cells while huFc and secondary detection antibody do not show any binding. Cells were incubated with 100 nM of Fcab/C-IgG for 60 min at 4 °C, washed twice with PBS-1 % BSA, incubated for 30 min with 500 nM of AF488-labeled detection antibody (109-546-008, Jackson ImmunoResearch) at 4 °C in darkness, washed twice with PBS-1 % BSA, and finally fluorescence intensity was measured applying an Attune NxT flow cytometer (Invitrogen™).

A



B

cell line	EGFR/cell	K_D [nM]		
		Fcab-1	Fcab-2	Fcab-3
MDA-MB-468	$\sim 1 \times 10^6$	2.58	2.59	2.40
A431	$\sim 0.7 \times 10^6$	1.50	1.84	1.75
MCF-7	-	-	-	-

Figure S5. Determination of cellular dissociation constants (K_D). **(A)** EGFR positive (MDA-MB-468 and A431) and EGFR negative (MCF-7) cells were incubated with Fcabs at different concentration followed by staining with AF488-labeled detection antibody, washing and cytometer analysis as described in Figure S4. Varying binding saturation levels between MDA-MB-468 and A431 cells reflect distinct cell specific EGFR expression densities. Dose response curves were fitted using the asymmetric (five parameter) fitting function of GraphPad Prism (GraphPad Software, Inc.) to obtain K_D . **(B)** Cellular dissociation constants of Fcabs are in good agreement with K_D values derived from binding to recombinant EGFR *via* BLI (Table 2) and literature data^[1].

5. Cellular uptake assay

For our cellular uptake study we used a pH-dependent fluorophore (pHAb-dye) based assay.^[2] We directly labeled constructs with pHAb-dye by applying random lysine coupling and acquired their intracellular accumulation kinetics on cells by measuring the fluorescence increase over time generated when constructs reach the acidic endosome and/or lysosome. Importantly, the fluorescence of randomly coupled pHAb-dye molecules could be altered by pHAb-dye local molecular environment (Figure S6C) probably resulting in a non-linear relationship between the number of coupled pHAb-dye molecules and the individual fluorescence of a construct.^[2-4] To consider this, we developed a method similar to Wang *et al.* to derive a fluorescence- and absorption-based degree of pHAb-dye labeling (DOL^F and DOL^A) from SE-HPLC data.^[5] The SE-HPLC method has the advantage to simultaneously analyze DOL^F and DOL^A as well as aggregation and purification (free pHAb-dye) status of the labeled construct. The DOL^F value of each pHAb-dye labeled construct can then be used to normalize fluorescence values of intracellular accumulation kinetics.

In the following a detailed description of the method is given. Figure S6D summarizes the method in short.

SE-HPLC analysis

SE-HPLC was performed on a 1260 Infinity device from Agilent Technologies equipped with a diode array (DAD) and a fluorescence (FLD) detector module and either a TSKgel SuperSW3000 or a SuperSW2000 column. The mobile phase consisted of 50 mM sodium phosphate, 400 mM sodium perchlorate, pH 6.3 and its flow rate was set to 0.35 mL/min. The DAD was set to detect absorption at 280 nm (aromatic amino acids) and 535 nm (pHAb-dye). The excitation and emission wavelengths of the FLD were set to 535 nm and 566 nm to record fluorescence of pHAb-dye (Figure S6B).

Free pHAb-dye, pHAb-dye conjugated proteins and the corresponding unconjugated proteins were then analyzed by SE-HPLC. Figure S7 depicts exemplarily the resulting chromatograms for unconjugated protein, free pHAb-dye and pHAb-dye conjugated protein. In a next step, the molar extinction or fluorescence coefficients were derived from these data.

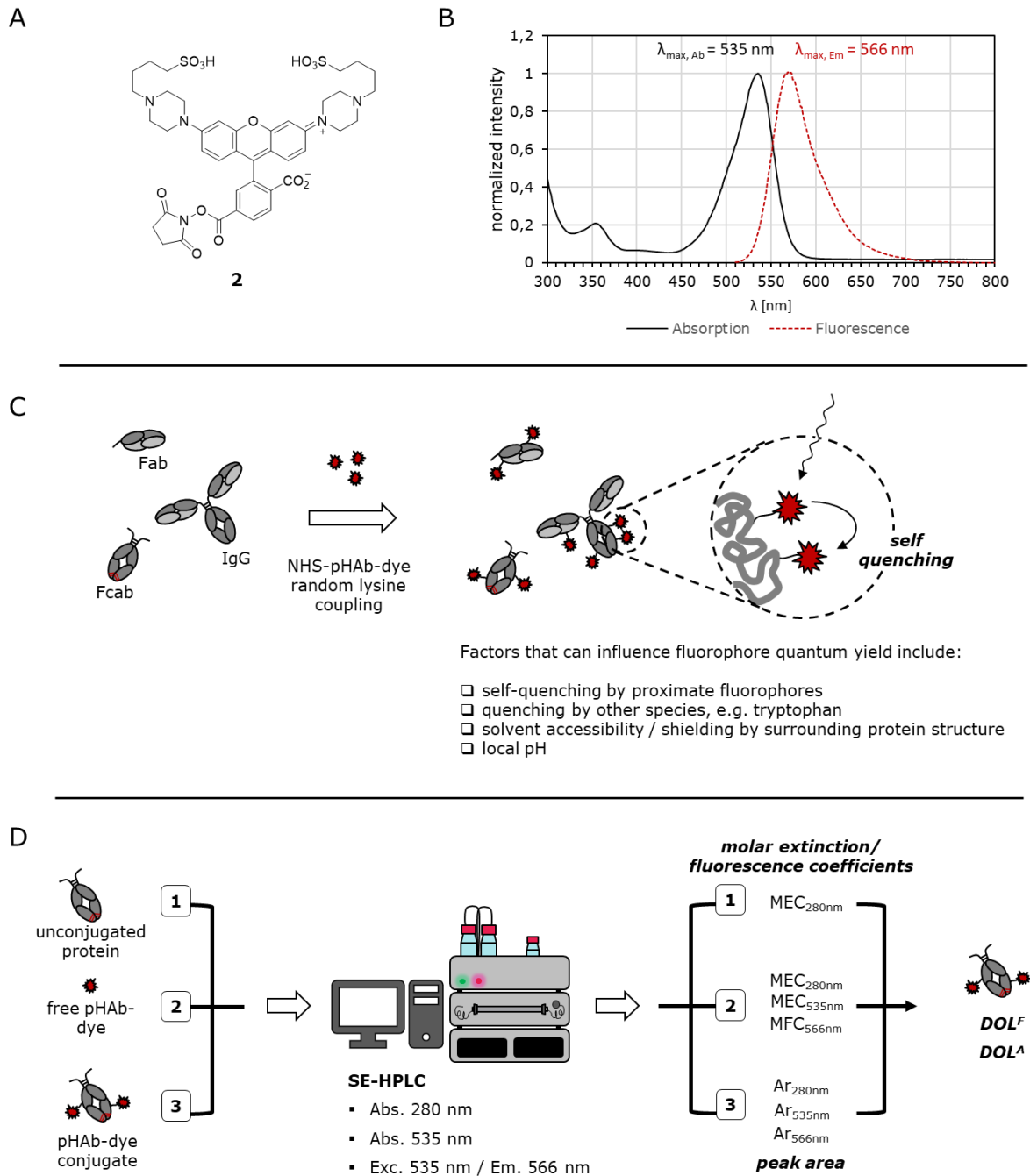


Figure S6. pHAb-dye labeling and degree of labeling (DOL^F , DOL^A) determination **(A)** Structure of pHAb amine reactive dye **2** carrying an NHS ester group which can react with the ϵ -amino group of lysine. **(B)** Absorption and fluorescence spectra of pHAb dye in SE-HPLC buffer (pH 6.3). **(C)** Proteins are labeled with pHAb-dye *via* random lysine coupling. Several factors can impact fluorophore quantum yield.^[4] **(D)** Overview of the established SE-HPLC method to determine the DOL^F and DOL^A value. Unconjugated proteins, free pHAb-dye and pHAb-dye conjugates were analyzed by an SE-HPLC device equipped with a diode array (DAD) and a fluorescence (FLD) detector. The molar extinction coefficients (MEC) of unconjugated protein and free pHAb-dye as well as the molar fluorescence coefficient (MFC) of free pHAb-dye were calculated from peak areas and the injected amount of substance. MEC and MFC were then used to calculate the amount of conjugated fluorescent pHAb-dye and the amount of protein from pHAb-dye conjugate peak areas. Finally, DOL^F and DOL^A can be derived from these data.

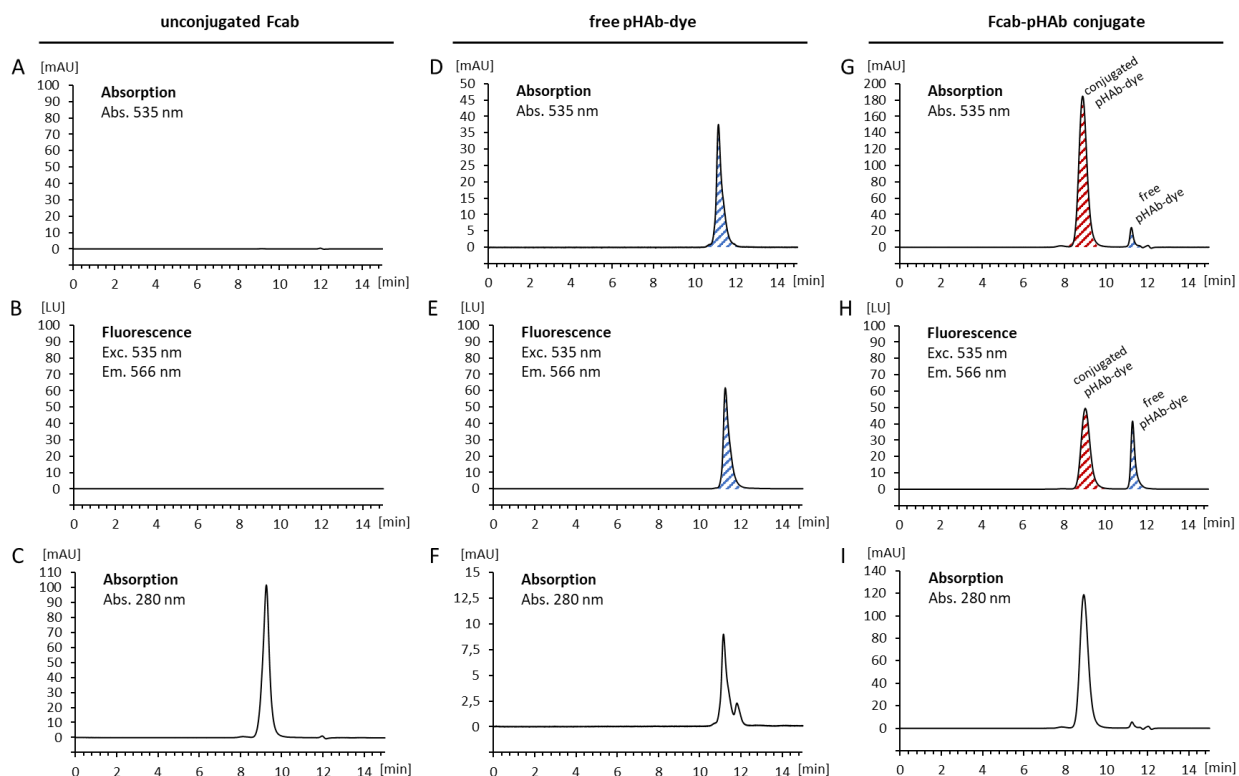


Figure S7. SE-HPLC analysis for the determination of the DOL^F and DOL^A , exemplarily shown for a pHAb-dye conjugated Fcab. **(A)** Unconjugated Fcab does not absorb light at 535 nm. **(B)** Hence, Fcab does not show fluorescence at 566 nm when excited at 535 nm (pHAb-dye absorption maximum). **(C)** Absorption of Fcab at 280 nm (aromatic amino acids). Fcab (54 kDa) elutes at 9.3 min. **(D)** Absorption of free pHAb-dye at its absorption maximum at 535 nm. According to its smaller size, free pHAb-dye (786 g/mol, carboxylic acid form) elutes later at 11.2 min. **(E)** Fluorescence at 566 nm (pHAb-dye fluorescence maximum) of free pHAb-dye when excited at 535 nm. **(F)** Free pHAb-dye absorbs also at 280 nm. The smaller peak at 11.8 min is caused by buffer components and was neglected for peak integration. **(G)** Absorption at 535 nm of Fcab-pHAb conjugate. The first peak marked in red represents the absorption of conjugated pHAb-dye molecules while the second peak marked in blue shows free pHAb-dye which could not be removed entirely by Zeba™ spin desalting column purification. **(H)** Fluorescence at 566 nm of Fcab-pHAb conjugate. The peak depicted in red shows fluorescence of conjugated pHAb-dye while the blue peak shows fluorescence of free pHAb-dye. When comparing the peak area of fluorescence and absorption peaks (535 nm), fluorescence of conjugated pHAb-dye is much lower with respect to free pHAb-dye. This confirms influences of the local molecular environment on fluorophore quantum yield. **(I)** Absorption of Fcab-pHAb at 280 nm is composed of the absorption of its protein and pHAb-dye components.

Calculating molar extinction / fluorescence coefficient (MEC/MFC) of unconjugated protein and free pHAb-dye from SE-HPLC peak area

MEC/MFC of unconjugated protein and free pHAb-dye were calculated from SE-HPLC peak areas. Exemplary chromatograms can be found in Figure S7C (unconjugated protein) and Figure S7D-F (free pHAb-dye). Relevant peaks were integrated using the ChemStation analysis software by Agilent. From the corresponding peak area, the MEC_{280nm} of the unconjugated protein and the $MEC_{535nm} / MFC_{566nm}$ of free pHAb-dye could be determined applying the following equation derived from Wang *et al.*^[5]

$$\varepsilon_i = \frac{Ar \cdot F}{l \cdot c \cdot v_{inj}} \quad (1)$$

where ϵ_i is the MEC or MFC at wavelength λ_i , Ar is the calculated peak area, F is the SE-HPLC flow rate, l is the flow cell path length, c is the concentration of the injected sample, and U_{inj} is the injected sample volume. Table S1 summarizes the resulting MEC and MFC of unconjugated proteins and free pHAb-dye.

Table S1. Molar extinction / fluorescence coefficient at different wavelengths. MEC and MFC are given as the mean \pm SD. Different volumes of unconjugated protein or free pHAb-dye solution were injected in three consecutive SE-HPLC runs and the resulting peak areas were used to calculate MEC or MFC from equation (1). For example, when injecting $v_{inj} = 7.5 \mu\text{L}$ of $c = 18.3 \mu\text{M}$ Fcab a single peak with a peak area Ar_{280nm} of 1825 eluted at 9.3 min (Figure S7C). With a constant SE-HPLC flow rate of $F = 5.8 \mu\text{L/s}$, a MEC_{280nm} of $77122 (\text{mM}\cdot\text{cm})^{-1}$ was calculated.

analyte	MEC_{280nm} [mM·cm] ⁻¹	MEC_{535nm} [mM·cm] ⁻¹	MFC_{566nm} [mM·cm] ⁻¹
Fcab-1	94582 \pm 685	-	-
Fcab-2	94608 \pm 1	-	-
Fcab-3	96964 \pm 155	-	-
huFc	75217 \pm 306	-	-
C-Fab	72828 \pm 26	-	-
C-IgG	107610 \pm 182	-	-
free pHAb-dye	14825 \pm 257	60813 \pm 823	103746 \pm 3003

Calculating the DOL^F and DOL^A from SE-HPLC peak area of pHAb-dye conjugated protein and MEC/MFC

To calculate the DOL^F value from a pHAb-dye labeled construct, the molar amount of conjugated fluorescent pHAb-dye ($n_{pHAb,566nm}$) and protein ($n_{protein,280nm}$) was calculated first. Therefore, pHAb-dye labeled constructs were analyzed by SE-HPLC and the absorption and fluorescence peak area of conjugated pHAb-dye (Figure S7G-H peaks marked in red), as well as peak area from absorption at 280 nm (Figure S7I) were calculated. Absorption at 280 nm is caused not only by the protein structure but also by the conjugated pHAb-dye (Figure S7F). To calculate the amount of injected protein from this peak, the peak area that is contributed by pHAb-dye must be subtracted. The portion of pHAb-dye absorption at 280 nm can be derived from its peak area at 535 nm (Ar_{535nm}) and subtracted from total peak area at 280 nm (Ar_{280nm}) as shown in equation (2)

$$Ar_{280nm,corrected} = Ar_{280nm} - \left(Ar_{535nm} \cdot \frac{MEC_{pHAb,280nm}}{MEC_{pHAb,535nm}} \right) \quad (2)$$

Subsequently, the amount of injected protein can be calculated from the corrected peak area ($Ar_{280nm,corrected}$) by equation (3)

$$n_{protein,280nm} = \frac{Ar_{280nm,corrected} \cdot F}{MEC_{protein,280nm}} \quad (3)$$

Similarly, the amount of conjugated fluorescent pHAb-dye can be calculated from the peak area of its fluorescence signal at 566 nm (Ar_{566nm}):

$$n_{pHAb,566nm} = \frac{Ar_{566nm} \cdot F}{MFC_{pHAb,566nm}} \quad (4)$$

The ratio between the amount of conjugated fluorescent pHAb-dye molecules and protein defines the DOL^F value for the individual fluorescence of a construct:

$$DOL^F = \frac{n_{pHAb,566nm}}{n_{protein,280nm}} \quad (5)$$

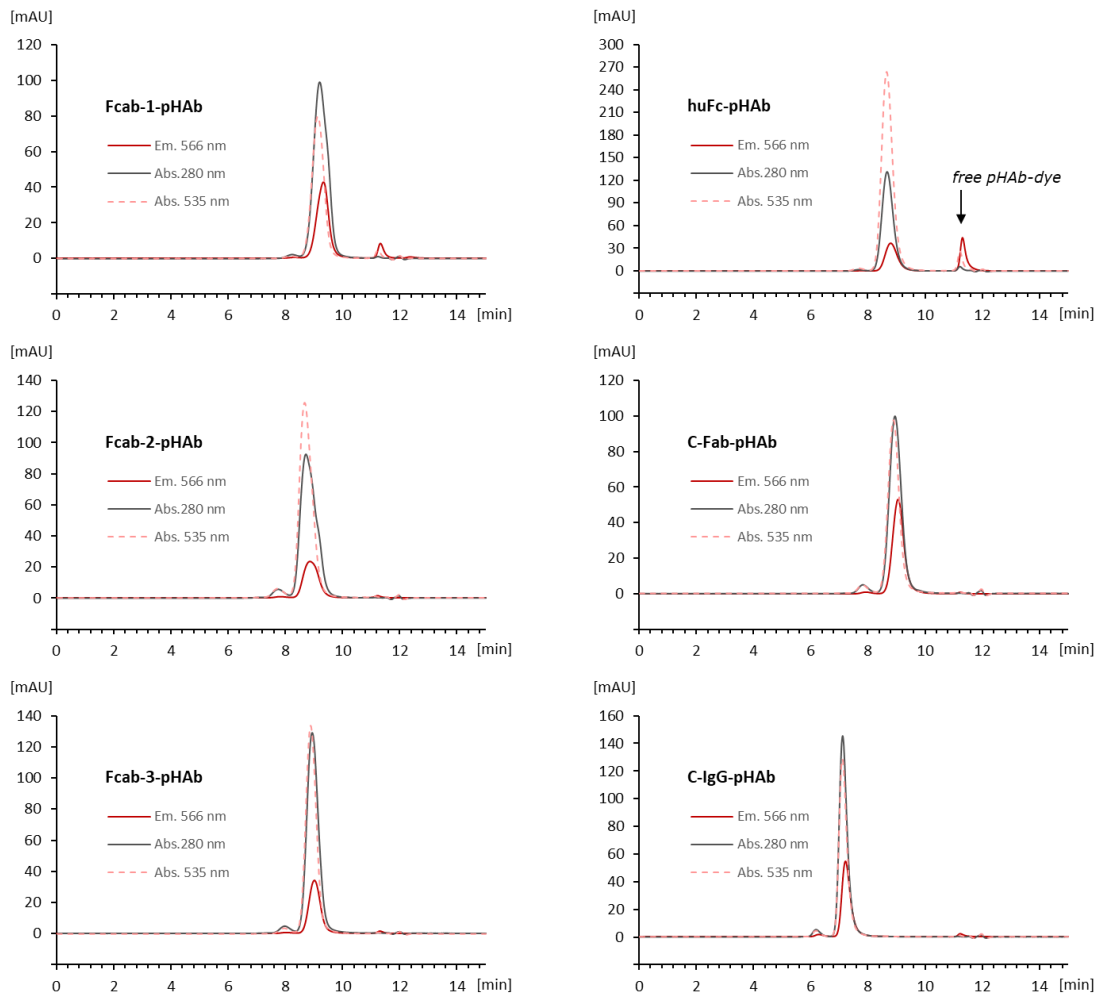
In analogy, the absolute amount of conjugated pHAb-dye molecules per protein (DOL^A) can be calculated from the peak area of pHAb-dye absorption at 535 nm applying equation (6) and (7).

$$n_{pHAb,535nm} = \frac{Ar_{535nm} \cdot F}{MEC_{pHAb,535nm}} \quad (6)$$

$$DOL^A = \frac{n_{pHAb,535nm}}{n_{protein,280nm}} \quad (7)$$

The SE-HPLC chromatograms of relevant pHAb-dye conjugates as well as DOL^F and DOL^A values are shown in Figure S8. In line with our expectations, the number of fluorescent pHAb-dye molecules per protein (DOL^F) is lower compared to the absolute number of conjugated pHAb-dye molecules (DOL^A). Since fluorescence represents the readout of the cellular uptake assay, fluorescence values can be normalized to their DOL^F value to account for the individual fluorescence of pHAb-dye labeled constructs. Consequently, the DOL^F and cell number normalized intracellular accumulation rates allow for comparability.

A



B

scaffold	pHAb-dye	
	DOL ^A	DOL ^F
Fcab-1-pHAb	1.26 ± 0.06	0.38 ± 0.03
Fcab-2-pHAb	2.28 ± 0.04	0.28 ± 0.02
Fcab-3-pHAb	1.93 ± 0.02	0.30 ± 0.01
huFc-pHAb	4.67 ± 0.02	0.41 ± 0.02
C-Fab-pHAb	1.36 ± 0.03	0.43 ± 0.00
C-IgG-pHAb	1.94 ± 0.05	0.51 ± 0.02

Figure S8. Characterization of pHAb-dye conjugates used in this study. **(A)** Analytical size exclusion SE-HPLC of purified pHAb-dye conjugates showing absorption at 280 nm (protein and pHAb-dye) and 535 nm (pHAb-dye) as well as pHAb-dye fluorescence (Exc. 535 nm, Em. 566 nm). At t_R 11 – 12 min unconjugated pHAb-dye may elute. **(B)** Absorption- and fluorescence-based degree of pHAb-dye labeling (DOL^F, DOL^A) derived from SE-HPLC data shown in (A).

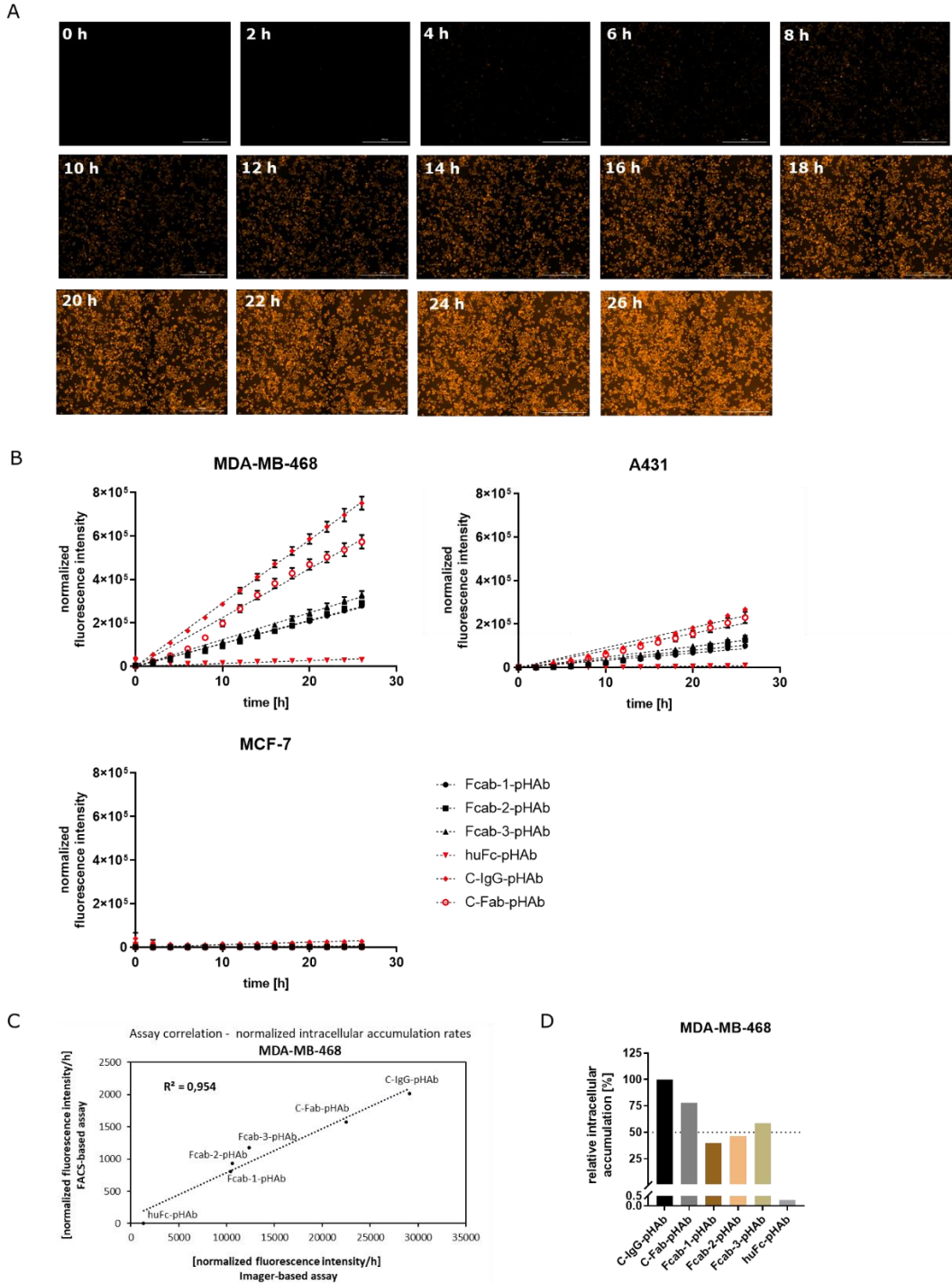


Figure S9. Cellular uptake kinetics of pHAb-dye labeled constructs. **(A)** Cellular accumulation time series exemplarily shown for Fcab-1-pHAb on MDA-MB-468 cells. Cells were incubated at 37 °C, 80 % humidity and 5 % CO₂ with 100 nM Fcab-1-pHAb and RFP channel images (ex.: 531 nm, em.: 593 nm) were recorded every 2 h for 26 h using a Cytation 5 cell imaging reader (BioTek) equipped with DAPI and RFP filter cubes and a BioSpa 8 automated incubator (BioTek). **(B)** The total fluorescence intensity of images is normalized to cell-number and DOL^F value of the pHAb-dye labeled construct and plotted over time to derive normalized intracellular accumulation rates from slopes of linear regression (GraphPad Software, Inc.). Subsequently, the relative intracellular accumulation can be calculated from these rates. **(C)** Normalized cellular uptake rates derived from described imager-based assay could be verified in a second FACS-based cellular uptake assay employing the same pHAb-dye labeled constructs. **(D)** Relative intracellular accumulation in MDA-MB-468 derived from FACS-based assay is in good agreement with the imaging-based cellular uptake data (Figure 1).

6. Generation of MMAE conjugates

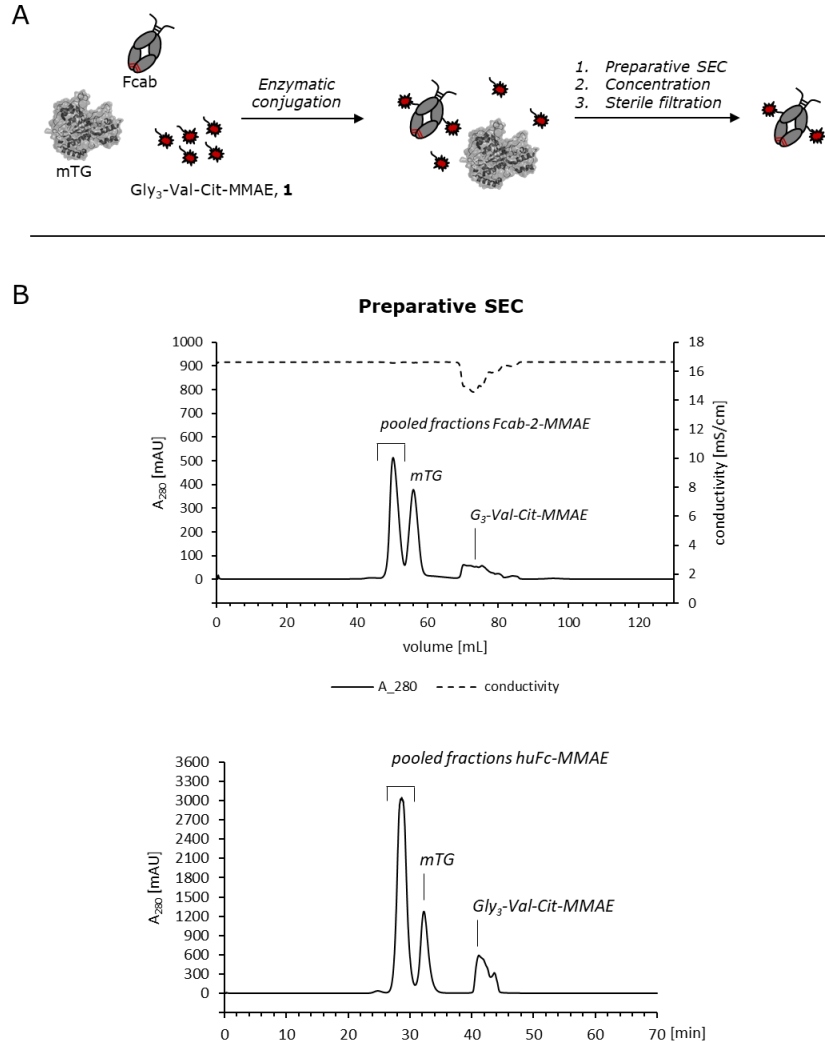


Figure S10. Conjugation and purification strategy exemplarily shown for Fcab-MMAE conjugates. **(A)** MMAE conjugates were generated by enzymatic transglutaminase conjugation. After conjugation, excess of microbial transglutaminase (mTG) and Gly₃-Val-Cit-MMAE (**1**) was removed by preparative SEC. **(B)** Purification of transglutaminase conjugated MMAE constructs by preparative SEC, exemplarily shown for Fcab-2-MMAE and huFc-MMAE. Fractions containing conjugated proteins (and non-conjugated species) were pooled, concentrated, sterile filtered and subjected to analytics.

7. Analytics of MMAE conjugates

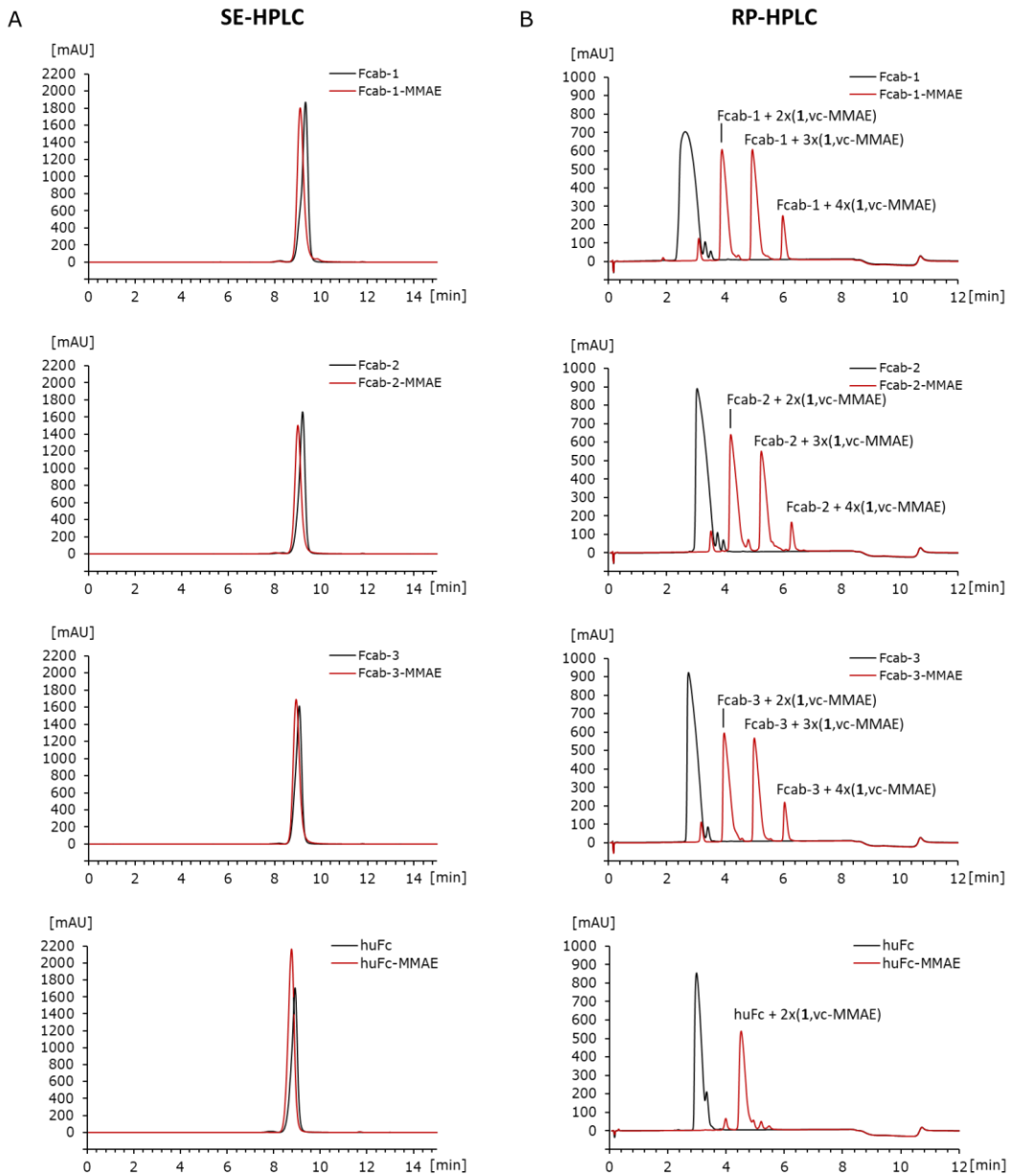
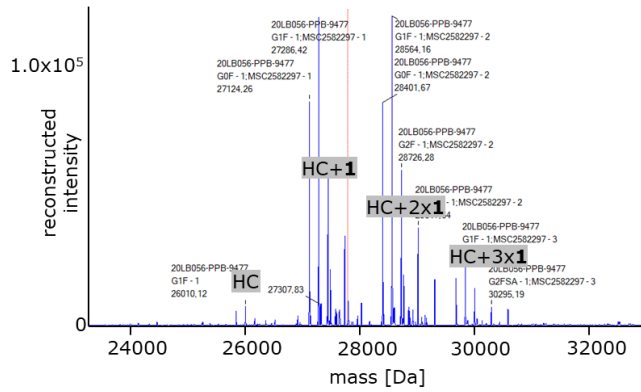


Figure S11. Chromatographic characterization of generated MMAE conjugates exemplarily shown for Fcab-1-MMAE, Fcab-2-MMAE, Fcab-3-MMAE and huFc-MMAE. **(A)** Analytical size exclusion SE-HPLC shows a distinct single peak demonstrating formation of monomeric drug conjugates without aggregates. Signal intensity represents absorption at 214 nm. **(B)** Reversed phase RP-HPLC reveals conjugation of Gly₃-Val-Cit-MMAE **1**. RP-DAR is calculated from peak areas of individual DAR species (Fcab-1-MMAE RP-DAR 2.6; Fcab-2-MMAE RP-DAR 2.5; Fcab-3-MMAE RP-DAR 2.5; huFc-MMAE RP-DAR 2.0). For example, 25 % relative peak area of DAR 1 species and 75 % relative peak area of DAR 2 species reveals a final RP-DAR of 1.75. Signal intensity represents absorption at 214 nm.

Table S2. Hydrophobic interaction chromatography (HI-HPLC) retention times (t_R) of unconjugated parental construct and DAR 1.0 – 3.0 MMAE-conjugate species. Relative retention time (RRT) refers to the ratio between the t_R of the DAR species indicated in the table below and the t_R of the unconjugated parental molecule. HI-HPLC RRT is an indicator for shielding of hydrophobic payloads such as MMAE and can be used to estimate the accessibility of linker-drugs for serum proteases like murine carboxylesterase.^[6]

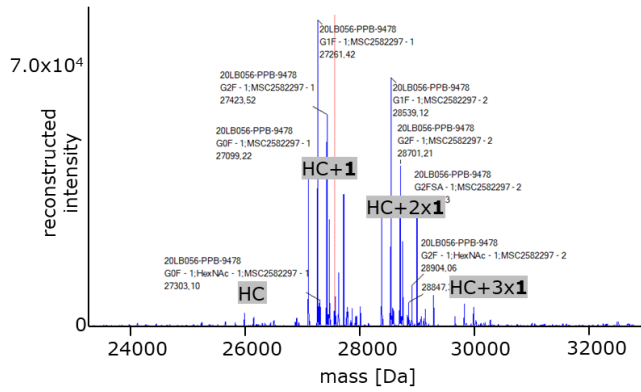
conjugate	HI-HPLC				RRT
	parental construct t_R [min]	DAR 1.0 conjugate t_R [min]	DAR 2.0 conjugate t_R [min]	DAR 3.0 conjugate t_R [min]	
Fcab-1-MMAE	15.66	15.63	17.07	17.95	1.15 (DAR 3.0)
Fcab-2-MMAE	13.34	13.48	15.11	15.91	1.19 (DAR 3.0)
Fcab-3-MMAE	12.42	12.53	14.18	15.13	1.22 (DAR 3.0)
huFc-MMAE	10.63	-	12.33	15.79	1.16 (DAR 2.0)
C-Fab-MMAE	7.89	12.90	-	-	1.63 (DAR 1.0)
C-IgG-MMAE	11.18	13.01	15.36	-	1.37 (DAR 2.0)

Fcab-1-MMAE



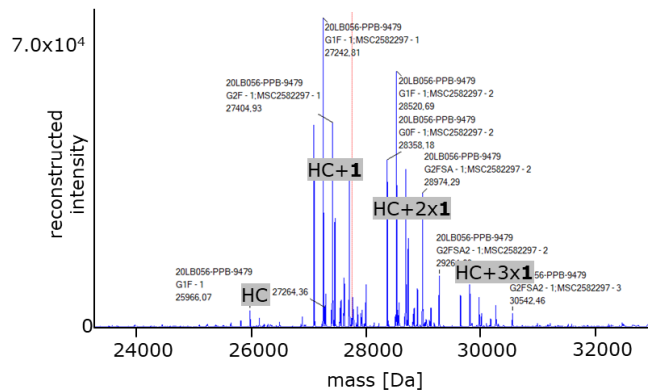
heavy chain + payload	glycosylation	most intense peak			TIC area [%]	MS-DAR
		calculated mass [kDa]	measured mass [kDa]	Δ mass [Da]		
HC	+G1F (+1607Da)	26.011	26.010	1	1.7	3.2
HC+1	+G1F (+1607Da)	27.289	27.286	3	43.8	
HC+2x1	+G1F (+1607Da)	28.568	28.564	4	45.1	
HC+3x1	+G1F (+1607Da)	29.846	29.842	4	9.4	

Fcab-2-MMAE



heavy chain + payload	glycosylation	most intense peak			TIC area [%]	MS-DAR
		calculated mass [kDa]	measured mass [kDa]	Δ mass [Da]		
HC	+G1F (+1607Da)	25.986	25.985	1	0.7	3.0
HC+1	+G1F (+1607Da)	27.264	27.261	3	52.8	
HC+2x1	+G1F (+1607Da)	28.543	28.539	4	43.4	
HC+3x1	+G1F (+1607Da)	29.822	29.816	6	3.0	

Fcab-3-MMAE



heavy chain + payload	glycosylation	most intense peak			TIC area [%]	MS-DAR
		calculated mass [kDa]	measured mass [kDa]	Δ mass [Da]		
HC	+G1F (+1607Da)	25.967	25.966	1	1.3	3.1
HC+1	+G1F (+1607Da)	27.245	27.243	2	49.6	
HC+2x1	+G1F (+1607Da)	28.524	28.521	3	41.4	
HC+3x1	+G1F (+1607Da)	29.802	29.798	4	7.8	

Figure S12. DAR determination of Fcab-MMAE conjugates by mass spectrometry. Deconvoluted MS spectra showing groups of differently glycosylated heavy chains (HC) carrying 0–3 Gly₃-Val-Cit-MMAE (**1**). TIC area of HC species carrying 0–3 linker payloads were used to calculate the MS-DAR.

8. Receptor binding properties of MMAE conjugates

Table S3. Kinetic parameters EGFR binding. Dissociation constants (K_D), on- (k_{on}) and off-rates (k_{off}) were measured at pH 7.4 by BLI using recombinantly produced EGFR. Errors are standard errors from fitting using FortéBio data analysis software 9.1. Fitting quality is characterized by R^2 .

	K_D [nM]	K_D error [nM]	k_{on} [$10^6/$ Ms]	k_{on} error [$10^6/$ Ms]	k_{off} [$10^{-3}/$ s]	k_{off} error [$10^{-3}/$ s]	full fitting R^2
Fcab-1	2.42	0.01	0.311	0.001	0.752	0.001	0.9995
Fcab-1-MMAE	2.67	0.02	0.346	0.002	0.924	0.003	0.9979
Fcab-2	1.07	0.01	0.371	0.001	0.397	0.001	0.9991
Fcab-2-MMAE	1.37	0.01	0.385	0.001	0.528	0.002	0.9991
Fcab-3	1.71	0.01	0.332	0.001	0.568	0.002	0.9991
Fcab-3-MMAE	1.54	0.01	0.405	0.001	0.622	0.001	0.9993
C-Fab	0.82	0.00	0.713	0.003	0.585	0.002	0.9995
C-IgG	1.25	0.01	1.172	0.008	1.462	0.004	0.9959
C-IgG-MMAE	0.60	0.01	1.451	0.012	0.868	0.004	0.9941
huFc	-	-	-	-	-	-	-

Table S4. Kinetic parameters FcRn binding. Dissociation constants (K_D), on- (k_{on}) and off-rates (k_{off}) were measured by BLI using recombinantly produced FcRn. Binding affinity to FcRn was determined at pH 6.0. Errors are standard errors from fitting using FortéBio data analysis software 9.1. Fitting quality is characterized by R^2 .

	K_D [nM]	K_D error [nM]	k_{on} [$10^6/$ Ms]	k_{on} error [$10^6/$ Ms]	k_{off} [$10^{-3}/$ s]	k_{off} error [$10^{-3}/$ s]	full fitting R^2
Fcab-1	381	12	0.292	0.007	111	2	0.9958
Fcab-1-MMAE	309	10	0.232	0.006	72	2	0.9971
Fcab-2	329	13	0.339	0.011	112	2	0.9954
Fcab-2-MMAE	362	12	0.210	0.005	76	2	0.9958
Fcab-3	589	22	0.289	0.009	170	3	0.9952
Fcab-3-MMAE	337	12	0.232	0.007	78	2	0.9964
C-IgG	747	24	0.219	0.006	164	2	0.9975
C-IgG-MMAE	892	31	0.185	0.006	165	3	0.9974

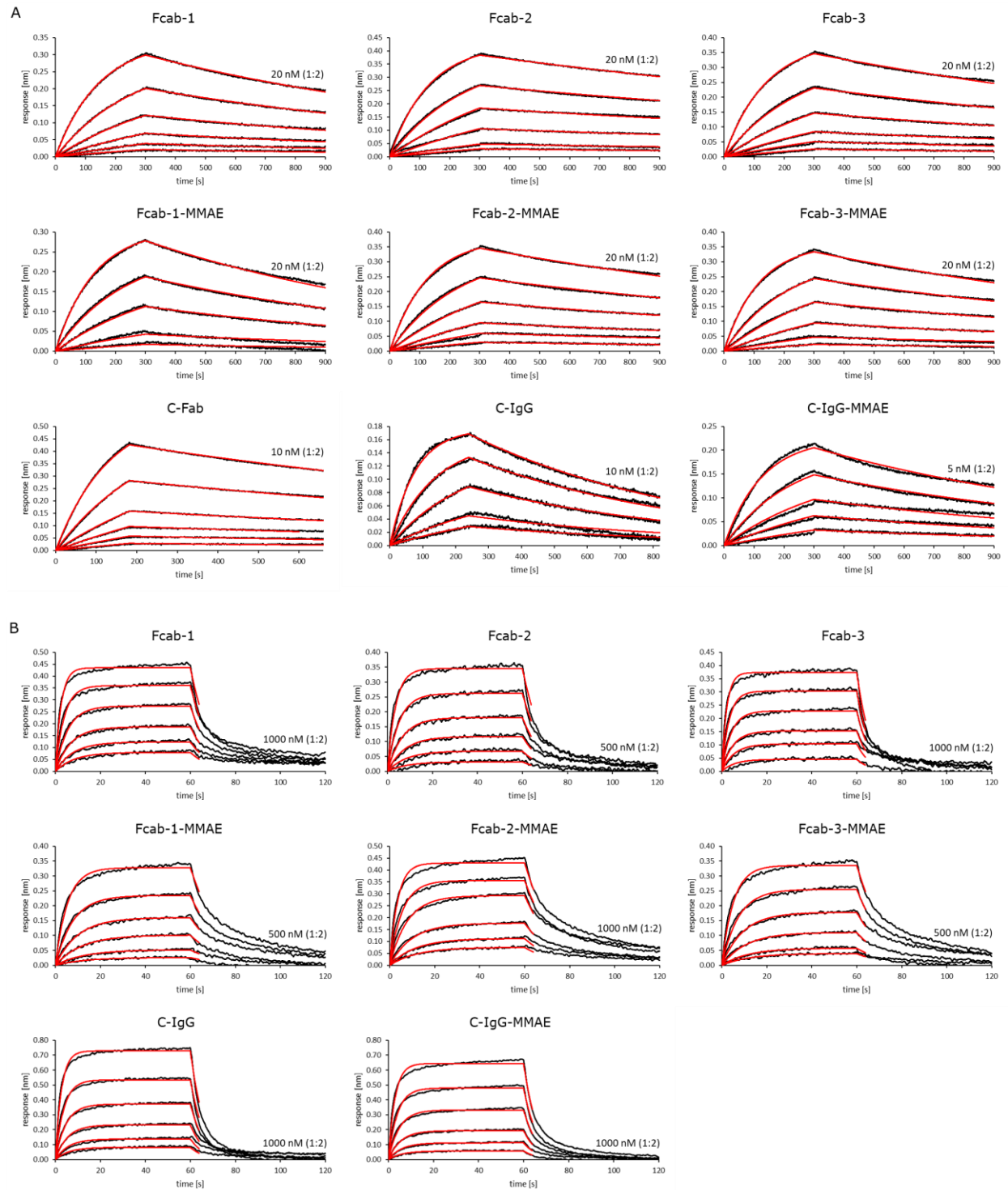


Figure S13. Receptor binding BLI sensorgrams of unconjugated Fcabs, Cetuximab variants and respective MMAE conjugates (A) EGFR binding analysis. Association and dissociation were recorded at pH 7.4 and fitted by a 1:1 global full-fit binding model. (B) FcRn binding analysis. Association and dissociation of analytes were recorded at pH 6.0 and fitted by a 1:1 global partial-dissociation model. Fittings are shown in red. For each sensorgram, the highest concentration of analyte during association and its dilution factor are given.

9. References

- [1] M. Tuna, K.-M. Leung, H. Sun, M. Medcalf, S. Isaac, *EGFR Binding Molecules*, **2018**, CA3030505A1.
- [2] N. Nath, B. Godat, C. Zimprich, S. J. Dwight, C. Corona, M. McDougall, M. Urh, *J. Immunol. Methods* **2016**, *431*, 11–21.
- [3] T. Riedl, E. Van Boxtel, M. Bosch, P. W. H. I. Parren, A. F. Gerritsen, *J. Biomol. Screen.* **2016**, *21*, 12–23.
- [4] ThermoFisher Scientific, in *Mol. Probes Handb.*, **2010**, pp. 6–7.
- [5] C. Wang, S. Chen, J. Caceres-Cortes, R. Y. C. Huang, A. A. Tymiak, Y. Zhang, *J. Chromatogr. A* **2016**, *1455*, 133–139.
- [6] L. N. Tumey, F. Li, B. Rago, X. Han, F. Loganzo, S. Musto, E. I. Graziani, S. Puthenveetil, J. Casavant, K. Marquette, T. Clark, J. Bikker, E. M. Bennett, F. Barletta, N. Piche-Nicholas, A. Tam, C. J. O'Donnell, H. P. Gerber, L. Tchistiakova, *AAPS J.* **2017**, *19*, 1123–1135.